Available online at www.sciencedirect.com
ScienceDirect
Journal of the European Ceramic Society 27 (2007) 3359–3364
www.elsevier.com/locate/jeurceramsoc

Hardness degradation in liquid-phase-sintered SiC with prolonged sintering

O. Borrero-López [a], A. Pajares [b], A.L. Ortiz [a], F. Guiberteau [a,*]

[a] *Departamento de Electrónica e Ingeniería Electromecánica, Escuela de Ingenierías Industriales, Universidad de Extremadura, 06071 Badajoz, Spain*
[b] *Departamento de Física, Facultad de Ciencias, Universidad de Extremadura, 06071 Badajoz, Spain*

Available online 1 May 2007

Abstract

The effect of the sintering time on the Vickers hardness of liquid-phase-sintered SiC with 10 wt% YAG additives was studied for materials fabricated in Ar and N_2 atmospheres. The hardness of the Ar-sintered materials was found to decrease markedly with increasing sintering time, whereas, in contrast, the decrease was only marginal for the N_2-sintered materials. Berkovich nanoindentation tests showed that the softening could not be attributed in either case to degradation of the SiC grains, thereby pointing to the intergranular YAG phase as the responsible. That the cause was degradation of the YAG phase was confirmed by X-ray energy-dispersive spectrometry and Hertzian indentation tests. The far more pronounced softening observed for the Ar-sintered materials reflects the more severe degradation that the YAG phase undergoes during sintering in this atmosphere.

Keywords: Liquid-phase sintering; SiC; Hardness; Mechanical properties

1. Introduction

Liquid-phase sintering is the most effective way of densifying silicon carbide (SiC) at a moderate processing temperature without the simultaneous application of external pressure,[1–8] and therefore at low cost. In this context, the most widely studied additive system for SiC is Y_2O_3–Al_2O_3, especially when these components are chosen in the form $Y_3Al_5O_{12}$. Typically, prolonged sintering in an Ar atmosphere is used to process such a liquid-phase-sintered (LPS) SiC to improve its long-crack toughness,[8–13] since the sintering duration promotes grain coarsening, and the crack-bridging toughening mechanism in LPS SiC is more efficient with increasing grain size.[14] However, it has been shown that LPS SiC resulting from prolonged sintering, the so-called "in situ toughened SiC", are much softer than those sintered for shorter times.[8,10,13,15] Whereas reduced hardness facilitates machining of LPS SiC parts, it can limit their utility in various structural applications. Although hardness degradation with prolonged sintering is a well-documented effect, to the best of the authors' knowledge no studies have explored the underlying causes of the phenomenon.

Thus, the present study was designed with two objectives in mind. The first was to evaluate the influence of the sintering atmosphere (Ar or N_2-gas) on the hardness degradation in LPS SiC with prolonged sintering. For this propose, we used exclusively Vickers indentation tests. Our results showed that the Vickers hardness is much more stable when the sintering is performed in an N_2 atmosphere. The second objective was to investigate the origin of the softening in the two atmospheres. To this end, we combined mechanical tests of Berkovich nanoindentation, which allows the evolution of the SiC grain hardness to be followed, and Hertzian indentation, which allows the progression of the interface weakness to be monitored through the yield stress values. The results point to intergranular phase degradation as being the key to the softening in both cases, as was also confirmed by direct X-ray energy-dispersive spectrometry.

2. Experimental procedure

2.1. Processing

α-SiC powder (UF-15, H.C. Starck, Goslar, Germany) with 4.29 wt% Al_2O_3 (AKP-30, Sumitomo Chemical Company, New York, NY, USA) and 5.71 wt% Y_2O_3 (Fine Grade, H.C. Starck, Goslar, Germany) as additives was ball-milled for 24 h in ethanol

* Corresponding author. Tel.: +34 924 28 9530; fax: +34 924 289601.
E-mail address: guiberto@unex.es (F. Guiberteau).

0955-2219/$ – see front matter © 2007 Elsevier Ltd. All rights reserved.
doi:10.1016/j.jeurceramsoc.2007.02.189

using ZrO_2 balls. This batch composition yields LPS SiC ceramics with 7.3 vol.% YAG after sintering. The slurry was dried, and the resulting powder deagglomerated and sieved. Compacts were made by uniaxial pressing (C, Carver Inc., Wabash, IN, USA) at 50 MPa, followed by isostatic pressing (CP360, AIP, Columbus, OH, USA) at 350 MPa. Sintering was performed (1000-3560-FP20, Thermal Technology Inc., Santa Rosa, CA, USA) at 1950 °C for 1–7 h in a flowing Ar- or N_2-gas atmosphere. Additional details of the processing procedure have been given elsewhere.[5,8,16] Surfaces for microstructural and mechanical characterizations were diamond-polished to 1 μm finish.

2.2. Microstructural characterization

Densities of the sintered ceramics were measured using the Archimedes method, with distilled water as the immersion medium. Cross-sections of all materials were plasma-etched (PT 1750, Fissions Instruments, East Sussex, UK), and were then observed under the SEM (S-3600N, Hitachi, Japan). Grain morphology analysis was performed from the SEM micrographs by image analysis on no less than 300 grains/ceramic. The nitrogen content in the N_2-sintered samples was measured using the inert gas (helium) fusion method (TNT-414, Leco Corporation, St. Joseph, MI, USA). Analysis of the chemical composition in selected samples was performed using the X-ray energy-dispersive spectrometer (XFLASH Detector 3001, Röntec GmbH, Germany) attached to the SEM.

2.3. Mechanical characterization

Vickers indentations were made (MV-1, Matsuzawa, Tokyo, Japan) at a load P of 98 N to measure the hardness of composites, determined[14] as $H_V = P/2d^2$, where d is the impression half-diagonal measured by optical microscopy. Ten separate indentations were performed on each material, and the mean of the measured values is reported here.

Nanoindentations were made (Micromaterials, Wrexham, UK) on selected composites using a Berkovich indenter (tip radius <100 nm) to measure the hardness of the constituents in these two-phase materials. Tests were conducted at variable load, such that the penetration depth was always 50 nm. Depth-sensing indentation hardness was evaluated from the indentation load–displacement curves, using the Oliver and Pharr method.[17,18] The hardness values reported here are the means of 100 indentations/sample.

Hertzian indentations were made (5535, Instron, Canton, MA, USA) using a tungsten carbide sphere of radius $r = 1.58$–7.94 mm, at peak loads in the interval $P = 15$–4000 N. Measurements of the contact radius a (made visible by first coating the specimen surfaces with a gold field) at each given load P and sphere radius r enabled indentation stresses, $p_0 = P/\pi a^2$, and indentation strains, a/r, to be calculated for the construction of the indentation stress–strain curves.[19–21] Indentation yield pressures p_Y were evaluated from the threshold indentation stresses at which the indentation data first deviated from linearity, and they were then used to calculate the yield stressses Y through the expression $Y = p_Y/1.1$ (see Fig. 1).

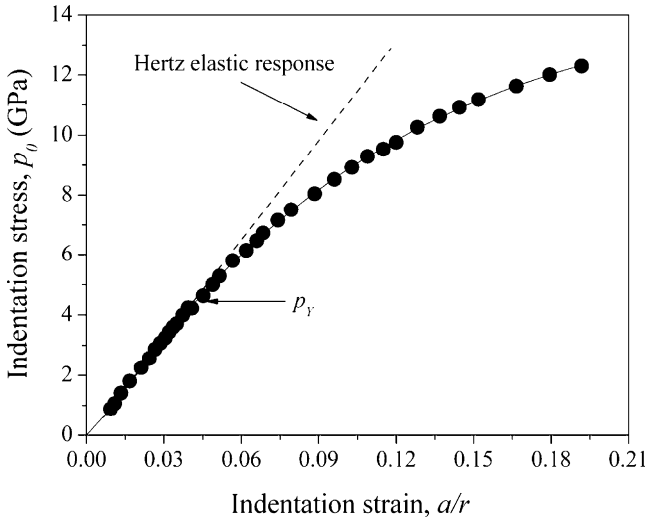

Fig. 1. Typical indentation pressure-strain curve at room-temperature for single-cycle Hertzian contacts in LPS SiC. The points are the experimental data for the material sintered for 1 h in the Ar atmosphere. The solid line through the data is a guide for the eye. The dashed line represents Hertzian-elastic response. The error bars for experimental data are lower than the point size.

3. Results and discussion

Fig. 2A–D shows SEM micrographs of the microstructures obtained for the extreme sintering times (1 and 7 h), in the two atmospheres. One observes that, consistent with the densities measured by the Archimedes method that indicated complete densification, the materials are pore free. With respect to the microstructure of the Ar-sintered materials, as shown in Fig. 3, up to 5-h sintering the grains have almost equiaxed form and sizes that increase with increasing sintering time. On the contrary, the 7-h sintered material contains both elongated and equiaxed grains, whose sizes are even larger than before (see Fig. 3). A detailed explanation of the microstructural evolution in LPS SiC fabricated in Ar atmosphere is given elsewhere.[16,22,23]

The grains in all the materials sintered in N_2 atmosphere have a nearly equiaxed form (aspect ratio 1.4), as shown in Fig. 3. With respect to the grain size, no appreciable change was observed with increasing sintering time, the value remaining within the ultrafine scale (see Fig. 3). The high viscosity of the liquid phase during sintering due to the incorporation of nitrogen from the atmosphere is the cause of the inhibition of grain growth mechanisms.[24] Indeed, we measured nitrogen contents of 0.3133 wt% and 0.6477 wt% after 1 h- and 7 h-sintering in the N_2 atmosphere. A detailed description of the microstructural evolution in LPS SiC fabricated in a N_2 atmosphere is given elsewhere.[24]

The hardness values obtained by Vickers indentation are shown in Fig. 4. One observes that the Ar- and N_2-sintered materials had similar hardnesses at 1 h-sintering, but the N_2-sintered materials were increasingly harder than their Ar-sintered counterparts with increasing sintering time. Furthermore, the hardness of the Ar-sintered materials decreased continuously by 5 GPa with increasing sintering time from 1 to 7 h, whereas the N_2-sintered materials decreased only marginally (by 1 GPa).

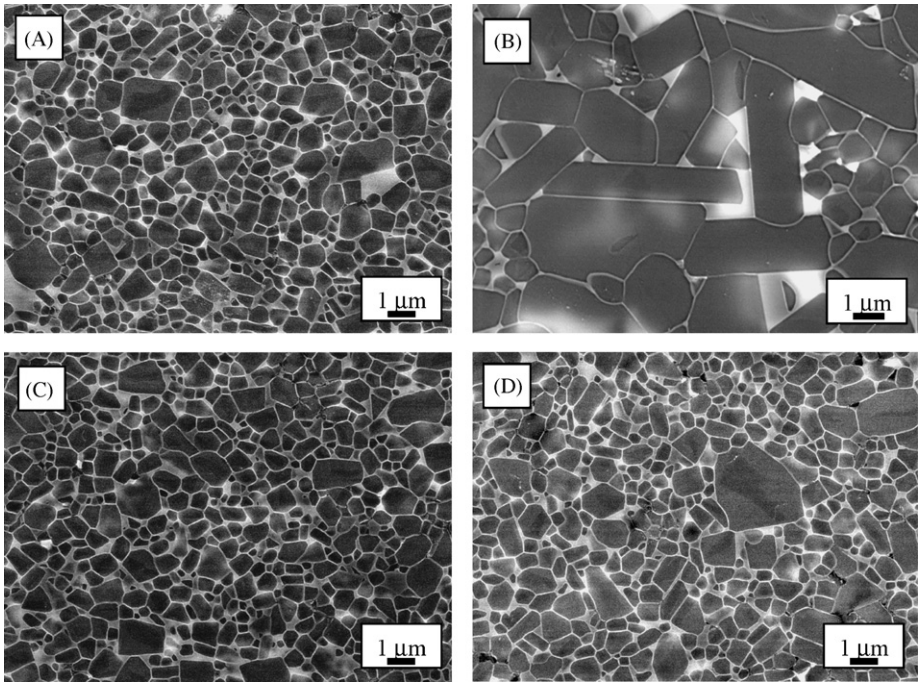

Fig. 2. SEM micrographs of LPS SiC processed for: (A) 1 h in Ar, (B) 7 h in Ar, (C) 1 h in N_2, and (D) 7 h in N_2. Dark regions are SiC grains and the light region is the YAG phase. Core-shell substructure within SiC grains is visible in the micrographs due to differential plasma-etching.

The experimentally observed softening of LPS SiC with prolonged sintering may be a consequence of the degradation of (1) the SiC grains, (2) the YAG phase, or (3) both. To elucidate the actual cause of the phenomenon, we performed Berkovich nanoindentation tests on the materials sintered for 1 and 7 h in the two atmospheres. The utility of these tests is that they are capable of evaluating (at least) the hardness of the SiC grains in the SiC/YAG composites due to the small size of the indents. The distributions of hardness values resulting from the tests are shown in Fig. 5A–D. Let us consider first the case of the Ar-sintered materials. One observes that the distribution for the 1-h material is centered at ~27 GPa, and that the range is 21–33 GPa. Furthermore, most of the indents lead to hardness values in the interval 25–31 GPa, which is the hardness range expected for the SiC grains.[25] The lower hardness values are therefore likely to arise from indents on mixed SiC/YAG zones, since the YAG phase is softer than the SiC phase and the thickness of the YAG phase is too small (<150 nm) to allow room for a clean indentation. The hardness distribution of the sample sintered for 7 h in an Ar atmosphere is broader (16–34 GPa) and shifted to higher hardness values (peak at ~31 GPa) compared to the 1-h case (see Fig. 5A and B). The heterogeneous microstructure of this ceramic is responsible for the greater dispersion in the hardness values. As was noted above, this material contains elongated SiC grains and a YAG phase located at the triple joints (Fig. 2B), not small grains surrounded completely by YAG phase. In this

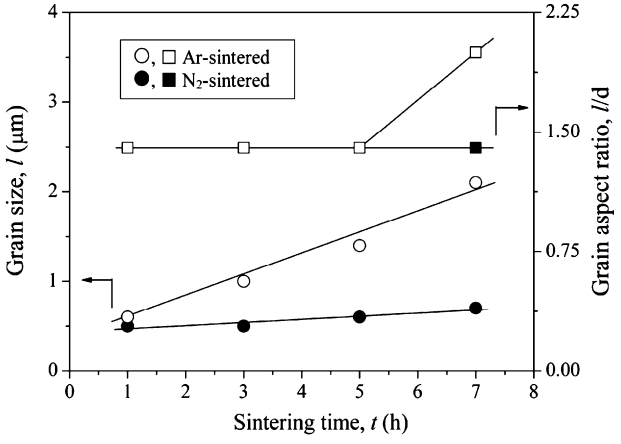

Fig. 3. Morphology of the SiC grains in LPS SiC as a function of the sintering time in Ar and N_2 atmospheres. Circles are for grain sizes and squares for grain aspect ratios. The solid lines are guides for the eye. The open and close squares overlap up to 5 h sintering time.

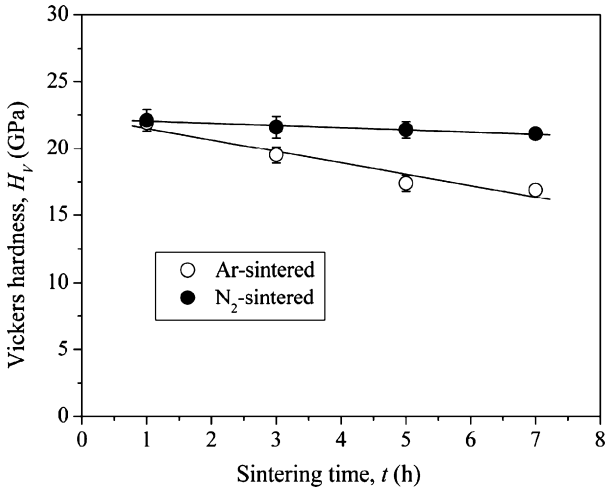

Fig. 4. Vickers hardness of LPS SiC as a function of the sintering duration in Ar and N_2 atmospheres. The solid lines are guides for the eye.

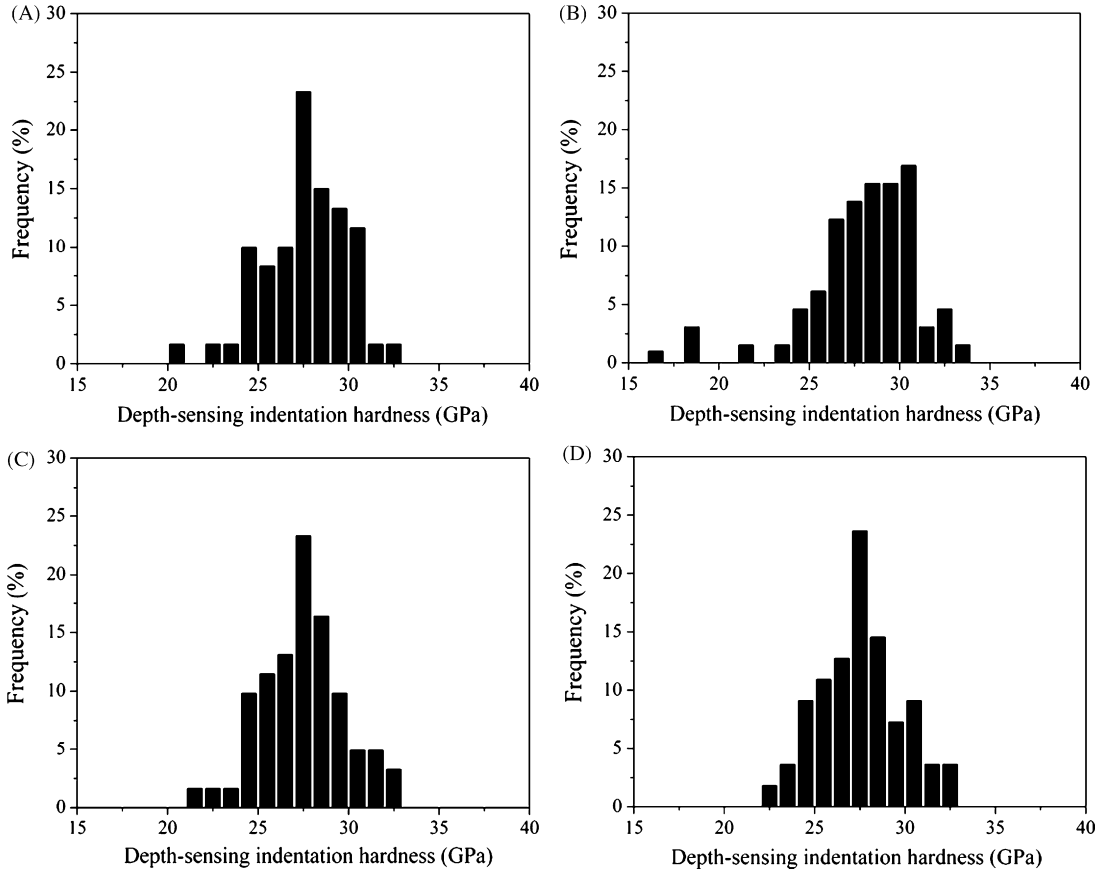

Fig. 5. Depth-sensing indentation hardness distributions measured by Berkovich nanoindentation tests on LPS SiC processed for: (A) 1 h in Ar, (B) 7 h in Ar, (C) 1 h in N_2, and (D) 7 h in N_2.

type of microstructure, one expects cleaner indents on the SiC grains and, occasionally, on the YAG pockets. With this in mind, we suggest therefore that the hardness values around 15 GPa come exclusively from indents on the YAG phase,[26] whereas the rest are from indents on SiC grains (25–34 GPa) or, to a lesser extent, on mixed SiC/YAG zones (20–25 GPa). The shift in the peak distribution to higher hardness values thus reflects the increased hardness of the SiC grains, which is attributed to the well-documented[27] solid-solution hardening.[c] Given this circumstance, the softening of LPS SiC is not due to degradation of the SiC grains, because they are indeed harder than before. Therefore, degradation of the YAG phase during the prolonged sintering at high temperatures is the cause of the reduction in the Vickers hardness of the SiC/YAG composites sintered in an Ar atmosphere. As shown in Fig. 6A, comparison of the EDS spectra of the extreme materials reveals the existence of modifications in the Al, Y, and O content, thereby providing direct evidence of the degradation of the YAG phase.

Now, consider the case of the N_2-sintered materials. As was seen above, there was only a marginal softening of the LPS SiC with N_2-sintering (see Fig. 4). Unlike the Ar-case, solid-solution hardening is in this case not likely to occur due to the inhibition of the grain growth mechanisms during N_2-sintering. Neither can the marginal hardness degradation be attributed to incorporation of nitrogen into the SiC grains due to its low solubility (~100 ppm)[24] and because N-doped SiC grains would be harder than their N-free counterparts. Both considerations are supported by the results from the nanoindentation tests, which again showed no evidence for changes in the distributions of the hardness values of the SiC grains (Fig. 5C and D). Once again, degradation of the YAG phase must thus be deemed responsible for the marginal softening of LPS SiC sintered in an N_2 atmosphere. However, this degradation is much less important than for the Ar-case, because the Vickers hardness remained almost unchanged after the longer sintering times. We suggest that the liquid phase obtained in an N_2 atmosphere is chemically more stable at the high sintering temperatures because the incorporation of nitrogen during the heat treatment makes it highly viscous and refractory. This would also explain why the SiC/YAG composites sintered in N_2 are harder than their Ar-sintered counterparts, despite the absence of a solid-solution hardening effect in the SiC grains. Similarly to the Ar-case, the EDS analyses shown in Fig. 6B confirm the existence of degradation of the YAG phase, but this time to a lesser extent than before.

[c] To explain the greater hardness of the SiC grains with the prolonged sintering, one should consider in detail the Ostwald ripening mechanism responsible for the grain growth in LPS SiC. During sintering, small amounts of yttrium, aluminum, and oxygen incorporate from the liquid phase into the SiC grain forming solid solutions.[15,28] This is confirmed by the typical core-shell substructure of the SiC grains, revealed by plasma etching (see Fig. 1A and B). Solid-solution hardening must thus be deemed responsible for the increased hardness.

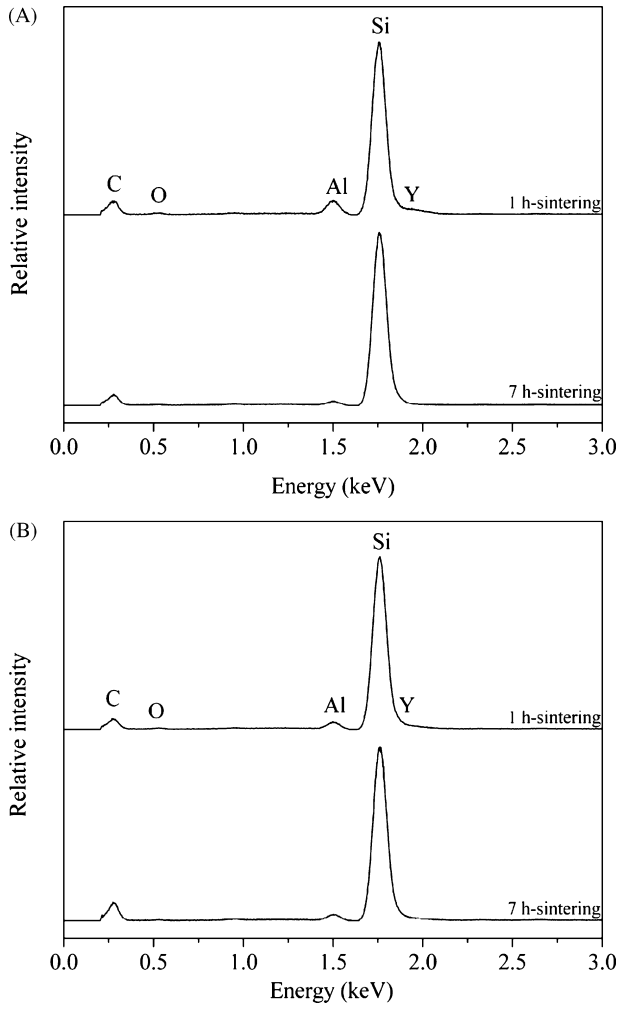

Fig. 6. Comparison of the EDS spectra of LPS SiC processed for 1 and 7 h in: (A) Ar, and (B) N_2 atmospheres.

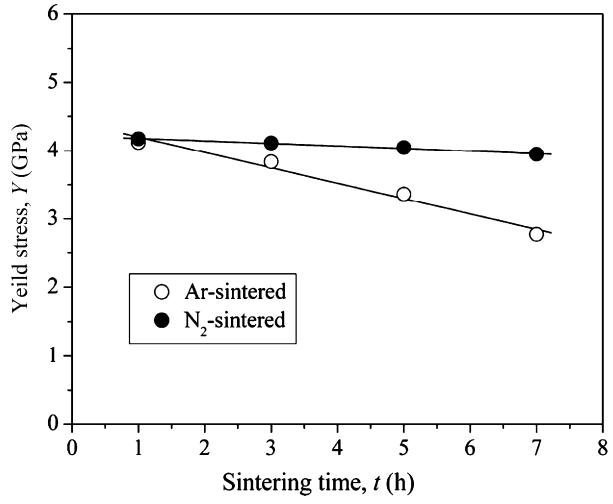

Fig. 7. Yield stress of LPS SiC as a function of the sintering duration in Ar and N_2 atmospheres. These values were determined by Hertzian indentation tests. The solid lines are guides for the eye.

To further confirm that the cause of the softening in the LPS SiC with prolonged sintering was the degradation of the YAG phase, we measured by Hertzian indentation the yield stress of our LPS SiC as a function of the sintering duration. The yield stress, which is defined as the minimum stress to cause plastic deformation, should decrease with increasing sintering duration if the YAG phase degrades. This is because the deviation from linearity in the Hertzian curve is due to quasi-plasticity in the form of shear faulting along the SiC/YAG interfaces. As seen in Fig. 7, the yield stress indeed did decrease continuously with increasing sintering duration, thus reflecting the higher interface weakness associated with the YAG degradation with prolonged sintering. Similarly to hardness case, the decrease in yield stress was more pronounced for the Ar-sintered than for the N_2-sintered materials, in good agreement with the severity of YAG degradation.

4. Conclusions

We here studied the effect of sintering time on the hardness of LPS SiC processed with 10 wt% YAG additives in Ar and N_2 atmospheres. Based on the results, the following conclusions can be drawn:

- The hardness of LPS SiC decreases severely with increasing sintering time in an Ar atmosphere, but only marginally when the sintering is performed in an N_2 atmosphere.
- Regardless of the sintering atmosphere, the softening of LPS SiC with prolonged sintering results from the degradation of the intergranular phase, not from degradation of the SiC grains.
- The severe softening that occurs in the Ar-sintered materials reflects the major degradation that the liquid phase undergoes during sintering in this atmosphere. The only minor softening observed in the N_2-sintered materials is because the corresponding liquid phase is less susceptible to degradation due to the incorporation of nitrogen during sintering.

Acknowledgements

This work was supported by the Ministerio de Ciencia y Tecnología (Government of Spain), the Fondo Europeo de Desarrollo Regional (FEDER) under grant nos. CICYT MAT 2004-05971 and UNEX00-23-013.

References

1. Suzuki, K. and Sasaki, M., Pressureless sintering of silicon carbide. In *Fundamental Structural Ceramics*, ed. S. Somiya and R. C. Bradt. Terra Scientific Publishing Company, Tokyo, Japan, 1987, pp. 75–87.
2. Omori, M. and Takei, H., Pressureless sintering of SiC. *J. Am. Ceram. Soc.*, 1982, **C92**, 65–69.
3. Negita, K., Effective sintering aids for silicon carbide ceramics: reactivities of silicon carbide with various additives. *J. Am. Ceram. Soc.*, 1986, **69**, C308–C310.
4. Mulla, M. A. and Krstic, V. D., Low-temperature pressureless sintering of β-silicon carbide with aluminum oxide and yttrium oxide additions. *Am. Ceram. Soc. Bull.*, 1991, **70**, 439–443.

5. Pujar, V. V., Jensen, R. P. and Padture, N. P., Densification of liquid-phase-sintered silicon carbide. *J. Mater. Sci. Lett.*, 2000, **19**, 1011–1014.
6. Winn, E. J. and Clegg, W. J., Role of the powder bed in the densification of silicon carbide sintered with yttria and alumina additions. *J. Am. Ceram. Soc.*, 1999, **82**, 3466–3470.
7. Mulla, M. A. and Krstic, V. D., Pressureless sintering of β-SiC with Al_2O_3 additions. *J. Mater. Sci.*, 1994, **29**, 934–938.
8. Padture, N. P., In situ-toughened silicon carbide. *J. Am. Ceram. Soc.*, 1994, **77**, 519–523.
9. Padture, N. P. and Lawn, B. R., Toughness properties of a silicon carbide with in situ-induced heterogeneous grain structure. *J. Am. Ceram. Soc.*, 1994, **77**, 2518–2522.
10. Borrero-López, O., Ortiz, A. L., Guiberteau, F. and Padture, N. P., Propiedades Mecánicas a Temperatura Ambiente de Cerámicos de α-SiC Sinterizados con Fase Líquida de Y_2O_3–Al_2O_3. *Bol. Soc. Esp. Ceram. Vidrio*, 2005, **44**, 265–269.
11. Borrero-Lopez, O., Ortiz, A. L., Guiberteau, F. and Padture, N. P., Effect of microstructure on sliding-wear properties of liquid-phase-sintered α-SiC. *J. Am. Ceram. Soc.*, 2005, **88**, 2159–2163.
12. Kim, Y. W., Lee, S. G. and Mitomo, M., Microstructural development of liquid-phase-sintered silicon carbide during annealing with uniaxial pressure. *J. Eur. Ceram. Soc.*, 2002, **22**, 1031–1037.
13. Baud, S. and Thevenot, F., Microstructures and mechanical properties of liquid-phase sintered seeded silicon carbide. *Mater. Chem. Phys.*, 2001, **67**, 165–174.
14. Lawn, B. R., *Fracture of Brittle Solids* (*2nd ed.*). Cambridge University Press, Cambridge, UK, 1993.
15. Borrero-Lopez, O., Ortiz, A. L., Guiberteau, F. and Padture, N. P., Improved sliding-wear resistance in in-situ toughened silicon carbide. *J. Am. Ceram. Soc.*, 2005, **88**, 3531–3534.
16. Xu, H., Bhatia, T., Deshpande, S. A., Padture, N. P., Ortiz, A. L. and Cumbrera, F. L., Microstructural evolution in liquid-phase-sintered SiC. Part I. Effect of starting SiC powder. *J. Am. Ceram. Soc.*, 2001, **84**, 1578–1584.
17. Oliver, W. C. and Pharr, G. M., An improved technique for determining hardness and elastic-modulus using load and displacement sensing indentation experiments. *J. Mater. Res.*, 1992, **7**, 1564–1583.
18. Fischer-Cripps, A. C., *Nanoindentation*. Springer-Verlag, New York, USA, 2002.
19. Guiberteau, F., Padture, N. P., Cai, H. and Lawn, B. R., Indentation fatigue—a simple cyclic Hertzian test for measuring damage accumulation in polycrystalline ceramics. *Philos. Mag. A*, 1993, **68**, 1003–1016.
20. Guiberteau, F., Padture, N. P and Lawn, B. R., Effect of grain size on Hertzian contact damage in alumina. *J. Am. Ceram. Soc.*, 1994, **77**, 1825–1831.
21. Ortiz, A. L., Muñoz-Bernabé, A., Borrero-López, O., Domínguez-Rodríguez, A., Guiberteau, F. and Padture, N. P., Effect of sintering atmosphere on the mechanical properties of liquid-phase-sintered SiC. *J. Eur. Ceram. Soc.*, 2004, **24**, 3245–3249.
22. Tanaka, H. and Zhou, Y., Low temperature sintering and elongated grain growth of 6H-SiC powder with AlB_2 and C additives. *J. Mater. Res.*, 1999, **14**, 519–522.
23. Tanaka, H., Hirosaki, N., Nishimura, T., Shin, D.-W. and Park, S.-S., Nonequiaxial grain growth and polytype transformation of sintered α-silicon carbide and β-silicon carbide. *J. Am. Ceram. Soc.*, 2003, **86**, 2222–2224.
24. Ortiz, A. L., Bhatia, T., Padture, N. P. and Pezzotti, G., Microstructural evolution in liquid-phase-sintered SiC. Part III. Effect of nitrogen-gas sintering atmosphere. *J. Am. Ceram. Soc.*, 2002, **85**, 1835–1840.
25. Richerson, D. W., *Modern Ceramic Engineering*. Marcel Dekker, New York, USA, 1992.
26. deWith, G. and Parren, J. E. D., Translucent $Y_3Al_5O_{12}$ ceramics: mechanical properties. *Solid State Ionics*, 1985, **16**, 87–93.
27. Mitchell, T. E. and Heuer, A. H., Solution hardening by aliovalent cations in ionic crystals. *Mater. Sci. Eng.*, 1997, **28**, 81–97.
28. Sigl, L. S. and Kleebe, H.-J., Core/rim structure of liquid-phase-sintered silicon carbide. *J. Am. Ceram. Soc.*, 1993, **76**, 773–776.